An effective rate equation approach to reaction kinetics in small volumes: Theory and application to biochemical reactions in nonequilibrium steady-state conditions

R. Grima

Citation: J. Chem. Phys. **133**, 035101 (2010); doi: 10.1063/1.3454685
View online: http://dx.doi.org/10.1063/1.3454685
View Table of Contents: http://jcp.aip.org/resource/1/JCPSA6/v133/i3
Published by the American Institute of Physics.

An effective rate equation approach to reaction kinetics in small volumes: Theory and application to biochemical reactions in nonequilibrium steady-state conditions

R. Grima[a)]
School of Biological Sciences, University of Edinburgh, Edinburgh EH9 3JR, United Kingdom

(Received 22 April 2010; accepted 26 May 2010; published online 16 July 2010)

Chemical master equations provide a mathematical description of stochastic reaction kinetics in well-mixed conditions. They are a valid description over length scales that are larger than the reactive mean free path and thus describe kinetics in compartments of mesoscopic and macroscopic dimensions. The trajectories of the stochastic chemical processes described by the master equation can be ensemble-averaged to obtain the average number density of chemical species, i.e., the true concentration, at any spatial scale of interest. For macroscopic volumes, the true concentration is very well approximated by the solution of the corresponding deterministic and macroscopic rate equations, i.e., the macroscopic concentration. However, this equivalence breaks down for mesoscopic volumes. These deviations are particularly significant for open systems and cannot be calculated via the Fokker–Planck or linear-noise approximations of the master equation. We utilize the system-size expansion including terms of the order of $\Omega^{-1/2}$ to derive a set of differential equations whose solution approximates the true concentration as given by the master equation. These equations are valid in any open or closed chemical reaction network and at both the mesoscopic and macroscopic scales. In the limit of large volumes, the effective mesoscopic rate equations become precisely equal to the conventional macroscopic rate equations. We compare the three formalisms of effective mesoscopic rate equations, conventional rate equations, and chemical master equations by applying them to several biochemical reaction systems (homodimeric and heterodimeric protein-protein interactions, series of sequential enzyme reactions, and positive feedback loops) in nonequilibrium steady-state conditions. In all cases, we find that the effective mesoscopic rate equations can predict very well the true concentration of a chemical species. This provides a useful method by which one can quickly determine the regions of parameter space in which there are maximum differences between the solutions of the master equation and the corresponding rate equations. We show that these differences depend sensitively on the Fano factors and on the inherent structure and topology of the chemical network. The theory of effective mesoscopic rate equations generalizes the conventional rate equations of physical chemistry to describe kinetics in systems of mesoscopic size such as biological cells. [doi:10.1063/1.3454685]

I. INTRODUCTION

The modeling of chemical reaction kinetics in the physical, chemical, and biological sciences has typically been approached through the construction and solution of a set of differential equations in the chemical concentrations of all species in the system. These equations are commonly referred to as rate equations (REs).[1,2] Even though they may not be analytically solvable in many cases of interest, their straightforward numerical solution gives quick insight into the chemical dynamics of the system and hence remains to this day a very popular choice. The use of these equations rests on two implicit assumptions: (i) the system evolves deterministically. Noise about the mean concentrations is proportional to $\Omega^{-1/2}$, where Ω is the volume of the compartment in which the reactions occur (also called the system size). Hence, the deterministic assumption is akin to assuming that the volume is very large such that the fluctuations can be safely ignored. (ii) The system is well-mixed via diffusion or constant stirring. This implies that there are no significant concentration gradients which hence justifies the nonspatial description of REs. Because of the first assumption, REs are also referred to as the macroscopic equations or the deterministic equations of chemical kinetics.

The use of REs as effective mathematical descriptions of kinetics is not unchallenged. At the microscopic scale, the time evolution of a system is much more faithfully captured by simulations based on molecular dynamics. The constant and meticulous tracking of the position and velocity of each molecule in the system is computationally very expensive, and hence a third approach has gained popularity and use in recent years. Chemical master equations (CMEs) are a mesoscopic stochastic description of chemical kinetics sitting between the microscopic regime of molecular dynamics and the macroscopic regime of REs.[3] It is far less computationally demanding than the former while relaxing the large

a)Electronic mail: ramon.grima@ed.ac.uk.

number of molecules requirement (or, equivalently, the large volume/deterministic assumption) of the latter. It is particularly useful in modeling biochemical reactions inside cells because of the naturally small number of interacting proteins (between a hundred to few thousands typically) in intracellular compartments.[2]

Over the past two decades, various methods have appeared, which generate realizations (or trajectories) of the stochastic chemical processes as described by CMEs; all of these numerical methods have been inspired by Gillespie's seminal contribution, the stochastic simulation algorithm (SSA).[4] In contrast, a general theoretical understanding of the effect of noise on kinetics is lacking, principally because CMEs do not lend themselves easily to analysis (e.g., steady-state analysis) as REs. One of the major tools in providing some understanding of this sort has been through the use of Van Kampen's linear-noise approximation,[5,6] which transforms a CME into a Fokker–Planck equation. The latter is a differential equation describing the time evolution of the probability density function of the noise about the macroscopic concentrations. The noise magnitude can then be estimated from the variance of the probability density function.

The linear-noise approximation method provides no corrections to the macroscopic concentrations as predicted by conventional REs. It only provides estimates of the noise about these concentrations. The trajectories generated by the SSA can be ensemble-averaged to obtain the average number density of chemical species, i.e., the true concentration, at any spatial scale of interest. These true concentrations are formally equal to the first moments of the probability distribution function of the system, i.e., the solution of the CME, divided by the volume of the compartment. Generally, the two concentrations, i.e., the macroscopic and true solutions, are either assumed to be the same or that differences are very small and hence negligible. However, recently, Grima[7,8] showed that these deviations can be very significant for an open system of a simple-enzyme-catalyzed reaction in an intracellular compartment. This suggests that at the mesoscopic scale, the time evolution of true concentrations is not governed by conventional REs but rather by a more general type of RE. The general derivation of these effective REs and their application to biochemical systems are the main topics of this paper.

This paper is divided as follows. In Sec. II, starting from a CME description of a completely general chemical reaction network, we derive the equation of motion for the joint probability density function of the system accurate to order $\Omega^{-1/2}$. This differential equation is shown to consist of the conventional Fokker—Planck equation plus new terms due to mesoscopic corrections. In Secs. III and IV, we use the latter equation to derive approximate time evolution equations for the mean number density of all chemical species in the system, valid at any volume. We refer to these equations as effective mesoscopic rate equations (EMREs). The conventional REs are shown to be special cases of the latter; more specifically in the limit of large volumes, EMREs reduce to REs but generally the former have new terms associated wit h novel kinetics only seen at the mesoscopic scale. In Sec. V, we apply these new equations to several examples of open biochemical systems whose steady-state is far from equilibrium. We conclude in Sec. VI with a general discussion.

II. TIME EVOLUTION EQUATION FOR THE PROBABILITY DENSITY FUNCTION OF A MESOSCOPIC CHEMICALLY REACTIVE SYSTEM

In this section we derive the equation of motion for the probability density function of a general system of reacting chemical species. Our derivation proceeds, broadly speaking, along the same lines as the elegant derivation of the general multidimensional linear-noise approximation by Elf and Ehrenberg.[6] However, note that in the present case we go beyond the linear-noise approximation.

Consider a system of N distinct chemical species interacting via R elementary reactions of the type

$$s_{1j}X_1 + \cdots + s_{Nj}X_N \xrightarrow{k_j} r_{1j}X_1 + \cdots + r_{Nj}X_N,$$

where j is an index running from 1 to R, X_i denotes species i, s_{ij} and r_{ij} are the stoichiometric coefficients, and k_j is the macroscopic rate constant of the reaction.

The macroscopic description is in terms of chemical concentrations. Denoting the concentration of species i by ϕ_i, the RE describing the kinetics of this system is given by

$$\frac{\partial \phi_i}{\partial t} = \sum_{j=1}^{R} (r_{ij} - s_{ij}) f_j(\vec{\phi}), \tag{1}$$

where $\vec{\phi}=(\phi_1,\ldots,\phi_N)^T$ is the vector of macroscopic concentrations. Each elementary reaction can at most involve the interaction of two species, and thus the macroscopic rate function, $f_j(\vec{\phi})$, can only be of four different forms: (i) a zeroth-order reaction by which a species is input into a compartment gives $f_j(\vec{\phi})=k_j$; (ii) a first-order unimolecular reaction involving the decay of some species h gives $f_j(\vec{\phi})=k_j\phi_h$; (iii) a second-order bimolecular reaction between two molecules of the same species h gives $f_j(\vec{\phi})=k_j\phi_h^2$; and (iv) a second-order bimolecular reaction between two molecules of different species, h and v, gives $f_j(\vec{\phi})=k_j\phi_h\phi_v$. Note that this functional form for f_j covers both the production and decay of species. We also note that all realistic models of chemical reactions can be decomposed into a series of elementary unimolecular and bimolecular reactions since three or more body collisions are rare.[3,5]

The mesoscopic description cannot be in terms of concentrations but rather in terms of $\vec{n}=(n_1,\ldots,n_N)^T$, which is the vector of the absolute number of molecules of each species. Intrinsic noise is increasingly important as the system size becomes smaller, and thus the mesoscopic description is necessarily probabilistic. The dynamics of the system can then be described by a partial differential equation for the probability P of being in state $\vec{n}$, an equation commonly known as the CME,[3,5]

$$\frac{\partial P(\vec{n},t)}{\partial t} = \Omega \sum_{j=1}^{R} \left(\prod_{i=1}^{N} E_i^{-S_{ij}} - 1 \right) \hat{f}_j(\vec{n},\Omega) P(\vec{n},t). \quad (2)$$

Note that Ω is the volume of the compartment in which the reactions occur and $S_{ij}=r_{ij}-s_{ij}$. The step operator $E_i^{-S_{ij}}$ is defined by its action on a general function g of the absolute number of molecules,

$$E_i^{-S_{ij}} g(n_1, \ldots, n_i, \ldots, n_N) = g(n_1, \ldots, n_i - S_{ij}, \ldots, n_N). \quad (3)$$

The microscopic rate function $\hat{f}_j(\vec{n},\Omega)$ has the general form

$$\hat{f}_j(\vec{n},\Omega) = k_j \prod_{z=1}^{N} \Omega^{-s_{zj}} \frac{n_z!}{(n_z - s_{zj})!}. \quad (4)$$

We note that the formalism used for the CME follows that of Van Kampen.[5] Gillespie[3] has a slightly different formalism, though the two are mathematically equivalent. In particular, in Van Kampen's style of presentation, there is an explicit factor of Ω and use is made of step operators in Eq. (2); another notable difference is that there is no extra factor in Eq. (4) to account for permutation symmetry for the case when reactants are identical, e.g., a homodimerization reaction.

The CME due to its inherent complexity is exactly solvable in only a few very simple cases. However, the dynamics it encapsulates can be systematically investigated by means of the system-size expansion due to Van Kampen.[5] The starting point of the method is to write the absolute number of molecules of species i as

$$\frac{n_i}{\Omega} = \phi_i + \Omega^{-1/2} \epsilon_i, \quad (5)$$

where ϕ_i is the macroscopic concentration of species i as determined by the RE [Eq. (1)] and ϵ_i is a continuous random variable whose statistical properties determine differences between the predictions of the RE and the CME. The ansatz [Eq. (5)] has the effect of transforming all functions of n_i into functions of the continuous random variable ϵ_i. We proceed with the expansion of the master equation by writing Eq. (2) in terms of the new variables. We will do this in three stages: first treating the time derivative on the left hand side of Eq. (2), then the step operator, and finally the microscopic rate function $\hat{f}_j$.

A. Time derivative

The variable change causes the probability distribution $P(\vec{n},t)$ to be transformed into a new one $\Pi(\vec{\epsilon},t)$, where $\vec{\epsilon}=(\epsilon_1,\ldots,\epsilon_N)^T$. The time derivative is then given by

$$\frac{\partial P(\vec{n},t)}{\partial t} = \frac{\partial \Pi(\vec{\epsilon},t)}{\partial t} + \sum_{i=1}^{N} \frac{\partial \epsilon_i}{\partial t} \frac{\partial \Pi(\vec{\epsilon},t)}{\partial \epsilon_i}$$

$$= \frac{\partial \Pi(\vec{\epsilon},t)}{\partial t} - \Omega^{1/2} \sum_{i=1}^{N} \frac{\partial \phi_i}{\partial t} \frac{\partial \Pi(\vec{\epsilon},t)}{\partial \epsilon_i}. \quad (6)$$

Note that the second step follows from the fact that the time derivative in the CME [Eq. (2)] is taken with constant molecule numbers which from Eq. (5) implies that $\partial \epsilon_i / \partial t = -\Omega^{1/2} \partial \phi_i / \partial t$.

B. Step operator

By using the definition of the step operator in Eq. (3), together with Eq. (5), it follows that

$$\prod_{i=1}^{N} E_i^{-S_{ij}} g(\epsilon_1, \ldots, \epsilon_i, \ldots, \epsilon_N)$$

$$= g(\epsilon_1 - \Omega^{-1/2} S_{1j}, \ldots, \epsilon_i - \Omega^{-1/2} S_{ij}, \ldots, \epsilon_N - \Omega^{-1/2} S_{Nj}). \quad (7)$$

The right hand side of the latter equation can now be written as a Taylor series from which it follows that the operator has the following formal expansion in powers of the inverse square root of the system volume:

$$\prod_{i=1}^{N} E_i^{-S_{ij}} - 1 = - \Omega^{-1/2} \sum_{i=1}^{N} S_{ij} \frac{\partial}{\partial \epsilon_i} + \frac{\Omega^{-1}}{2} \sum_{i,k=1}^{N} S_{ij} S_{kj} \frac{\partial^2}{\partial \epsilon_i \partial \epsilon_k}$$

$$- \frac{\Omega^{-3/2}}{6} \sum_{i,k,r=1}^{N} S_{ij} S_{kj} S_{rj} \frac{\partial^3}{\partial \epsilon_i \partial \epsilon_k \partial \epsilon_r}$$

$$+ O(\Omega^{-2}). \quad (8)$$

C. The microscopic rate function

The function $\hat{f}_j(\vec{n},\Omega)$ can take one out of four different forms depending on whether the jth elementary reaction is zeroth-order, unimolecular, bimolecular with same species and bimolecular between different species. We now consider these different forms for the microscopic rate function and express each one of them as a sum involving the macroscopic rate functions $f_j(\vec{\phi})$. These summation forms will then be shown to be special cases of a universal form which links the microscopic and macroscopic rate functions for all types of elementary reactions. Using Eqs. (4) and (5) and comparing with the macroscopic rate functions f_j [these have been discussed just after Eq. (1)], we have the following four cases.

Case (i). Zeroth-order, i.e., $s_{hj}=0$, $\forall h$,

$$\hat{f}_j(\vec{n},\Omega) = k_j = f_j(\vec{\phi}). \quad (9)$$

Case (ii). Unimolecular involving some species h, i.e., $s_{hj}=1$, $s_{zj}=0$ for $z \neq h$,

$$\hat{f}_j(\vec{n},\Omega) = k_j \frac{n_h}{\Omega} = k_j(\phi_h + \Omega^{-1/2} \epsilon_h)$$

$$= f_j(\vec{\phi}) + \Omega^{-1/2} \sum_{w=1}^{N} \epsilon_w \frac{\partial f_j(\vec{\phi})}{\partial \phi_w}. \quad (10)$$

Case (iii). Bimolecular involving same species h, i.e., $s_{hj}=2$, $s_{zj}=0$ for $z \neq h$,

$$\hat{f}_j(\vec{n},\Omega) = k_j \frac{n_h}{\Omega}\frac{n_h-1}{\Omega}$$
$$= k_j(\phi_h + \Omega^{-1/2}\epsilon_h)(\phi_h + \Omega^{-1/2}\epsilon_h - \Omega^{-1})$$
$$= k_j(\phi_h^2 + 2\Omega^{-1/2}\phi_h\epsilon_h + \Omega^{-1}(\epsilon_h^2 - \phi_h) - \Omega^{-3/2}\epsilon_h)$$
$$= f_j(\vec{\phi}) + \Omega^{-1/2}\sum_{w=1}^{N}\epsilon_w\frac{\partial f_j(\vec{\phi})}{\partial\phi_w}$$
$$+ \frac{\Omega^{-1}}{2}\sum_{w=1}^{N}(\epsilon_w^2 - \phi_w)\frac{\partial^2 f_j(\vec{\phi})}{\partial\phi_w^2} + O(\Omega^{-3/2}). \quad (11)$$

Case (iv). Bimolecular involving species h and v, i.e., $s_{hj}=s_{vj}=1$, $s_{zj}=0$ for $z\neq h,v$,

$$\hat{f}_j(\vec{n},\Omega) = k_j \frac{n_h}{\Omega}\frac{n_v}{\Omega}$$
$$= k_j(\phi_h + \Omega^{-1/2}\epsilon_h)(\phi_v + \Omega^{-1/2}\epsilon_v)$$
$$= k_j(\phi_h\phi_v + \Omega^{-1/2}(\phi_h\epsilon_v + \phi_v\epsilon_h) + \Omega^{-1}\epsilon_h\epsilon_v)$$
$$= f_j(\vec{\phi}) + \Omega^{-1/2}\sum_{w=1}^{N}\epsilon_w\frac{\partial f_j(\vec{\phi})}{\partial\phi_w}$$
$$+ \frac{\Omega^{-1}}{2}\sum_{w,z=1}^{N}\epsilon_w\epsilon_z\frac{\partial^2 f_j(\vec{\phi})}{\partial\phi_w\,\partial\,\phi_z}. \quad (12)$$

Hence, it can be deduced that all chemically plausible possible forms of $\hat{f}_j(\vec{n},\Omega)$ [i.e., Eqs. (9)–(12)] can be described by just one single general equation,

$$\hat{f}_j(\vec{n},\Omega) = f_j(\vec{\phi}) + \Omega^{-1/2}\sum_{w=1}^{N}\epsilon_w\frac{\partial f_j(\vec{\phi})}{\partial\phi_w}$$
$$+ \frac{\Omega^{-1}}{2}\left(\sum_{w,z=1}^{N}\epsilon_w\epsilon_z\frac{\partial^2 f_j(\vec{\phi})}{\partial\phi_w\,\partial\,\phi_z} - \sum_{w=1}^{N}\phi_w\frac{\partial^2 f_j(\vec{\phi})}{\partial\phi_w^2}\right)$$
$$+ O(\Omega^{-3/2}). \quad (13)$$

This equation expresses the microscopic rate functions in terms of the macroscopic ones.

The CME in terms of the new variables ϵ_i and the macroscopic rate functions f_j are then obtained by substituting Eqs. (6), (8), and (13) into Eq. (2). The resulting equation simplifies by noting that substitution of the macroscopic RE [Eq. (1)] cancels terms of the order of $\Omega^{1/2}$, leaving us with a series expansion in powers of $\Omega^{-1/2}$,

$$\frac{\partial\Pi}{\partial t} = -\sum_{i,w=1}^{N}J_{iw}\frac{\partial}{\partial\epsilon_i}(\epsilon_w\Pi) + \frac{1}{2}\sum_{i,k=1}^{N}D_{ik}\frac{\partial^2}{\partial\epsilon_i\,\partial\,\epsilon_k}\Pi$$
$$- \frac{\Omega^{-1/2}}{2}\left(\sum_{i,w,z=1}^{N}\frac{\partial J_{iw}}{\partial\phi_z}\frac{\partial}{\partial\epsilon_i}(\epsilon_w\epsilon_z\Pi) - \sum_{i,w=1}^{N}\phi_w\frac{\partial J_{iw}}{\partial\phi_w}\frac{\partial}{\partial\epsilon_i}\Pi\right)$$
$$- \frac{\Omega^{-1/2}}{6}\sum_{i,k,r=1}^{N}D_{ikr}\frac{\partial^3}{\partial\epsilon_i\,\partial\,\epsilon_k\,\partial\,\epsilon_r}\Pi + O(\Omega^{-1}), \quad (14)$$

where

$$J_{iw} = \sum_{j=1}^{R}S_{ij}\frac{\partial f_j(\vec{\phi})}{\partial\phi_w}, \quad (15)$$

$$D_{ik\cdots r} = \sum_{j=1}^{R}S_{ij}S_{kj}\cdots S_{rj}f_j(\vec{\phi}). \quad (16)$$

Note that Eq. (14) is defined in terms of the stoichiometric constants and macroscopic rate functions; this means that it can be straightforwardly constructed from the deterministic REs, a very convenient advantage as we shall see later on. Note also that J_{iw} are elements of the Jacobian matrix and $D_{ik\cdots r}$ are elements of a generalized diffusion matrix. Equation (14) is an approximate time evolution equation for the probability density function at mesoscopic volumes and is the main result of this section. The first two terms in this equation are the same as appear in the conventional Fokker–Planck equation and the last two terms encapsulate corrections due to small volumes. The linear-noise approximation of CMEs refers to the system-size expansion truncated to order Ω^0,[5] i.e., it corresponds to a Fokker–Planck approximation to the CME. Hence, Eq. (14) describes kinetic phenomena beyond that which can be captured using the linear-noise approximation. These novel effects are investigated in the rest of this article.

III. DERIVATION OF EFFECTIVE MESOSCOPIC REs

In this section we utilize the new time evolution equation for the probability density function of the system [Eq. (14)] to derive EMREs, i.e., approximate time evolution equations for the true concentrations. These will be different than the conventional REs since the latter describes the time evolution of macroscopic concentrations. We start by deriving equations for the first and second moments of the probability density function $\Pi(\vec{\epsilon},t)$. Multiplying both sides of Eq. (14) by ϵ_l and integrating over all ϵ_i $(i=1,\ldots,N)$ leads to

$$\frac{\partial\langle\epsilon_l\rangle}{\partial t} = \sum_{w=1}^{N}J_{lw}\langle\epsilon_w\rangle + \frac{\Omega^{-1/2}}{2}\left(\sum_{w,z=1}^{N}\frac{\partial J_{lw}}{\partial\phi_z}\langle\epsilon_w\epsilon_z\rangle - \sum_{w=1}^{N}\phi_w\frac{\partial J_{lw}}{\partial\phi_w}\right)$$
$$+ O(\Omega^{-1}), \quad (17)$$

where the angled brackets denote the mean. Similarly, multiplying both sides of Eq. (14) by $\epsilon_g\epsilon_l$ and integrating over all ϵ_i, one obtains the equation of motion for the second moments,

$$\frac{\partial\langle\epsilon_g\epsilon_l\rangle}{\partial t} = \sum_{w=1}^{N}J_{gw}\langle\epsilon_w\epsilon_l\rangle + J_{lw}\langle\epsilon_w\epsilon_g\rangle + D_{gl} + O(\Omega^{-1/2}). \quad (18)$$

These two equations can be compactly rewritten in matrix form as

$$\frac{\partial\langle\vec{\epsilon}\rangle}{\partial t} = \mathbf{J}\cdot\langle\vec{\epsilon}\rangle + \Omega^{-1/2}\vec{\Delta}(\mathbf{C}) + O(\Omega^{-1}), \quad (19)$$

$$\frac{\partial \mathbf{C}}{\partial t} = \mathbf{J}\cdot\mathbf{C} + \mathbf{C}\cdot\mathbf{J}^T + \mathbf{D} + O(\Omega^{-1/2}), \tag{20}$$

where $\mathbf{J}$ is the Jacobian matrix, $\langle\vec{\epsilon}\rangle = (\langle\epsilon_1\rangle, \ldots, \langle\epsilon_N\rangle)^T$ is the vector of the first moments, $\vec{\Delta}$ is a column vector whose lth entry is equal to the coefficient of $\Omega^{-1/2}$ in Eq. (17), and $\mathbf{C}$ and $\mathbf{D}$ are symmetric matrices with entries in the ith row and jth column equal to $\langle\epsilon_i\epsilon_j\rangle$ and D_{ij}, respectively. Note that the term $\vec{\Delta}(\mathbf{C})$ in Eq. (19) denotes evaluation of the vector $\vec{\Delta}$ using the entries of matrix $\mathbf{C}$ as obtained from the solution of Eq. (20).

The number density of species i, denoted as ϕ_i^R, is given by the quantity $\langle n_i/\Omega\rangle$. This is the formal definition of the true concentration. By averaging Eq. (5), we get an explicit expression relating the vector of true concentrations, $\vec{\phi}^R = (\langle n_1\rangle/\Omega, \ldots, \langle n_N\rangle/\Omega)^T$, and the vector $\langle\vec{\epsilon}\rangle$,

$$\vec{\phi}^R = \vec{\phi} + \Omega^{-1/2}\langle\vec{\epsilon}\rangle. \tag{21}$$

Solving the above equation for $\langle\vec{\epsilon}\rangle$ and substituting into Eq. (19), we finally obtain the EMREs for the system,

$$\frac{\partial \vec{\phi}^R}{\partial t} = \frac{\partial \vec{\phi}}{\partial t} + \mathbf{J}\cdot\left(\vec{\phi}^R - \vec{\phi}\right) + \Omega^{-1}\vec{\Delta}(\mathbf{C}) + O(\Omega^{-3/2}), \tag{22}$$

$$\frac{\partial \mathbf{C}}{\partial t} = \mathbf{J}\cdot\mathbf{C} + \mathbf{C}\cdot\mathbf{J}^T + \mathbf{D} + O(\Omega^{-1/2}). \tag{23}$$

Note that the solution of the EMRE depends on the solution of the RE. Note also that in the limit of large volumes, the third term in Eq. (22) tends to zero, which consequently implies that in the macroscopic limit, the EMRE reduces to the RE, i.e., the true concentration equals the macroscopic concentration. Generally, for finite volumes, the solution of the EMRE is different than that of the RE: inspection of Eqs. (19) and (20) shows that this nonequivalence stems from a coupling of the mean and the variance/covariance of intrinsic noise.

A. Computation of the vector $\vec{\Delta}$

From the above definition of $\vec{\Delta}$, it follows that the lth component of the vector is given by

$$\Delta_l = \frac{1}{2}\left(\sum_{w,z=1}^{N}\frac{\partial J_{lw}}{\partial \phi_z}\langle\epsilon_w\epsilon_z\rangle - \sum_{w=1}^{N}\phi_w\frac{\partial J_{lw}}{\partial \phi_w}\right). \tag{24}$$

We now evaluate the explicit forms which this equation can take by considering the most common types of elementary reactions which can compose a chemical reaction network. This will enable us to construct a simple look-up table which one can use to easily and quickly construct the vector $\vec{\Delta}$ for any reaction network, independent of its complexity or the number of interacting species.

The vector $\vec{\Delta}$ is defined in terms of the second derivatives of the macroscopic rate functions since

TABLE I. Contribution to the vector element Δ_l due to an elementary reaction involving species l with macroscopic rate constant k. Note that " " on the right-hand side of the reaction implies any species other than those appearing on the left-hand side of the reaction.

Zeroth-order	$\varnothing \to mX_l$	0
Unimolecular	$X_h \to X_l$	0
	$X_l \to \cdots + X_h + \cdots$	0
Bimolecular	$X_l + X_l \to X_h + \cdots$	$-2k[\langle\epsilon_l^2\rangle - \phi_l]$
	$X_h + X_h \to X_l + \cdots$	$k[\langle\epsilon_h^2\rangle - \phi_h]$
	$X_h + X_l \to X_v + \cdots$	$-k\langle\epsilon_l\epsilon_h\rangle$
	$X_h + X_v \to X_l + \cdots$	$k\langle\epsilon_h\epsilon_v\rangle$

$$\frac{\partial J_{lw}}{\partial \phi_i} = \sum_{j=1}^{R} S_{lj}\frac{\partial^2 f_j}{\partial \phi_i\,\partial\,\phi_w}. \tag{25}$$

Each elementary reaction that involves species l, as a reactant or as the product of a reaction, will contribute to Δ_l through the associated macroscopic rate function, as follows.

If the reaction is zeroth-order, for example, the injection of a certain species h in bursts of m molecules into the compartment, i.e., $\varnothing \to mX_h$ with macroscopic rate function $f_j = k_j$, then the second-order derivative of f_j is zero, and hence such a reaction provides NO contribution to Δ_l.

If the reaction is unimolecular, then either a molecule of species l is formed by the decay of a molecule of some other species h, i.e., $X_h \to X_l$ with macroscopic rate function $f_j = k_j\phi_h$ or a molecule of l decays to form one of another species h, i.e., $X_l \to X_h$ with macroscopic function $f_j = k_j\phi_l$ or else a molecule of l decays to form two molecules of the same species h or of different species h and v i.e. $X_l \to 2X_h$ or $X_l \to X_h + X_v$ with macroscopic function $f_j = k_j\phi_l$. In all three cases, the second derivative of f_j with respect to any macroscopic concentration variable is zero, and hence from Eqs. (24) and (25), one deduces that such a unimolecular reaction provides NO contribution to Δ_l.

If the reaction is bimolecular with same species, then either two molecules of species l dimerize to form one of species h, i.e., $X_l + X_l \to X_h$ with macroscopic function $f_j = k_j\phi_l^2$ or else two molecules of some species h dimerize to form one of species l, i.e., $X_h + X_h \to X_l$ with $f_j = k_j\phi_h^2$. In both cases, the second derivative of the macroscopic rate function is nonzero. Substituting the latter and the relevant stoichiometric constants into Eq. (25), one deduces from Eq. (24) that the respective contributions of the two possible types of bimolecular reaction between same species to Δ_l are equal to $-2k_j(\langle\epsilon_l^2\rangle - \phi_l)$ and $k_j(\langle\epsilon_h^2\rangle - \phi_h)$.

Lastly, if the reaction is bimolecular with different species, then either a molecule of species l reacts with one of species h to form a third different type v, i.e., $X_l + X_h \to X_v$ with macroscopic function $f_j = k_j\phi_l\phi_h$ or species l is produced as the product of the reaction between species h and v, i.e., $X_h + X_v \to X_l$ with $f_j = k_j\phi_h\phi_v$. In both cases, the second derivative of the macroscopic rate function is nonzero and the respective contributions to Δ_l are found to be equal to $-k_j\langle\epsilon_l\epsilon_h\rangle$ and $k_j\langle\epsilon_h\epsilon_v\rangle$. All the results are summarized in Table I. Note that the contribution to Δ_l from more complex elementary reaction steps, for example, those consistent with

the Lindemann mechanism (e.g., $X_l + X_h \rightarrow X_v + X_h$), can be straightforwardly deduced by a similar line of reasoning as for the cases treated in this section.

IV. CALCULATION PROCEDURE FOR STEADY-STATE SOLUTION OF EMRE

In Sec. III we derived the EMREs for a general reaction network. Though these equations are valid at any point in time, in the rest of this paper we will consider exclusively kinetics in steady-state conditions. Analysis of the transients and the approach to equilibrium is a considerably intricate study in its own and is treated in a separate forthcoming article.

Imposing steady-state conditions by setting the time derivatives in Eq. (22) to zero, we obtain

$$\mathbf{J} \cdot (\vec{\phi}^R - \vec{\phi}) = -\Omega^{-1}\vec{\Delta}(\mathbf{C}). \tag{26}$$

Note that the matrices $\mathbf{J}$ and $\mathbf{C}$ are also evaluated at steady-state. It follows immediately from the results of the previous section and Eq. (26) that any species i, which is involved purely in a number of unimolecular reactions, will have equal true and macroscopic concentrations, i.e., $\phi_i^R = \phi_i$. If a species is involved in at least one bimolecular reaction, then generally the two concentrations will not be equal.

For calculation purposes, the steady-state analysis can conveniently be divided into two stages. The first stage enables one to deduce which species will exhibit a true concentration, which is different than the macroscopic prediction. This stage requires very little computation and gives compact analytical expressions even for complex networks; this is very useful for getting an overall qualitative picture of the effects of noise on different parts of the reaction network. The second stage of the calculation involves the explicit calculation of the magnitude of the differences between the steady-state true and macroscopic concentrations. This leads to analytic expressions for simple networks but generally it is more suited as a numerical method to quantitatively explore the effects of small volumes on reaction kinetics. For ease of calculation, we now present a short, step-by-step, summary of the two stages.

A. Stage 1: Qualitative analysis of the effects of noise on the reaction network

(1) Identify the set of R elementary unimolecular and bimolecular reactions composing the reaction network of N interacting chemical species and then write the corresponding deterministic model. Using these equations compute the Jacobian matrix $\mathbf{J}$.

(2) For each species l, consider which elementary reactions it is involved in, and using the dictionary in Table I, construct the vector element Δ_l. Iterating this procedure for all N chemical species, one obtains the $N \times 1$ vector $\vec{\Delta}$.

(3) If the determinant of the Jacobian is nonzero, then compute the $N \times 1$ column vector: $\vec{\phi}^R - \vec{\phi} = -\Omega^{-1}\mathbf{J}^{-1} \cdot \vec{\Delta}(\mathbf{C})$. Note that up until this point there is no explicit evaluation of the elements of matrix $\mathbf{C}$, i.e., the steady-state correlators of the system, $\langle \epsilon_i \epsilon_j \rangle$, are left in algebraic form. The singular Jacobian case, for example, stemming from a number of implicit conservation laws, is treated by first computing Eq. (26) and then rewriting the resultant equations in terms of linearly independent quantities.

(4) Deduce which entries of the vector $\vec{\phi}^R - \vec{\phi}$ are zero. If the lth entry is zero, then the steady-state true concentration of the lth species is equal to the steady-state macroscopic concentration as predicted by the deterministic model. In contrast, a nonzero value indicates differences between the two concentrations in the limit of small volumes. The magnitude of these differences is estimated by the next stage of the method.

B. Stage 2: Quantitative analysis of the effects of noise on the reaction network

(1) Using the deterministic model for the chemical network deduce the stoichiometric constants and the set of macroscopic rate functions $f_j(\vec{\phi})$ (where j takes values from $1, \ldots, R$) for all elementary reactions. Use these to build the $N \times R$ stoichiometric matrix $\mathbf{S}$ whose elements are $S_{ij} = r_{ij} - s_{ij}$ and the $R \times R$ diagonal matrix $\mathbf{F}$ whose diagonal elements are $f_j(\vec{\phi})$.

(2) Compute the diffusion matrix $\mathbf{D} = \mathbf{S} \cdot \mathbf{F} \cdot \mathbf{S}^T$. Note that this expression is exactly equal to Eq. (16) with just two subscript indices; this result was derived by Elf and Ehrenberg[6] and provides a convenient means of computing the diffusion matrix from sole knowledge of the deterministic equations.

(3) Using the Jacobian and diffusion matrices, solve the Lyapunov equation $\mathbf{J} \cdot \mathbf{C} + \mathbf{C} \cdot \mathbf{J}^T + \mathbf{D} = 0$ for the symmetric matrix $\mathbf{C}$. This matrix gives all the steady-state correlators of the system, $\langle \epsilon_i \epsilon_j \rangle$, where indices i and j take values from $1, \ldots, N$. Note that a wide variety of efficient numerical methods are available to solve Lyapunov equations (see, for example, Refs. 9 and 10) including a fast implementation in MATLAB's control system toolbox.

(4) Substitute the required entries of $\mathbf{C}$ into the expression for the vector, $\vec{\phi}^R - \vec{\phi}$, as determined in step (3) of stage 1. Since the macroscopic solution $\vec{\phi}$ is known, we finally have the steady-state solution of the EMRE, i.e., $\vec{\phi}^R$.

V. STEADY-STATE MESOSCOPIC ANALYSIS OF OPEN SYSTEMS

We now illustrate the practical application of the method to chemical and biochemical systems of varying complexity. Such systems could in theory be closed or open; we choose to focus on open systems since a large variety of natural phenomena can be described as stationary states of such systems. An open system is one which can exchange matter with its environment, i.e., in our case, it means that there exist mechanisms for injecting and extracting molecules from the compartment in which the chemical or biochemical reactions are occurring.

The simplest choice is that molecules are injected independently at random points in time and also extracted independently.[5] A variety of other choices are possible and physically realizable. One mechanism which has been suggested by Van Kampen[5] and which has been studied by a few authors[6,8] is burst injection, i.e., molecules are injected m at a time into a compartment, while extraction occurs independent of each other. Grima[8] argued that such a process can effectively model the input of molecules into intracellular compartments when the molecules are transported to the compartments via active mechanisms of transport. Such a mechanism typically involves the packaging of a number of molecules in a vesicle or a granule, which is then transported along microtubules to a compartment wherein they are released.[11] In this article, we shall also use this mechanism for injecting molecules into our system but, of course, the application of the EMRE can be generally carried out for any mechanism of choice. Feeding m molecules at a time into a compartment will naturally enhance the size of the fluctuations, i.e., increase the variance of intrinsic noise. From Eq. (26), it follows that the size of the difference between the steady-state mesoscopic concentration and the corresponding macroscopic prediction is proportional to the variance and covariance of the noise, which suggests that the deviations of the predictions of EMREs from REs will increase with the burst input size m, i.e., the deviations will be dictated by how open is the system under consideration: the larger the exchange of matter, the larger the deviations. In the examples that follow, we show through explicit calculation that this principle indeed holds for a wide variety of biochemical systems.

A. Homodimerization: Bimolecular reactions between same species

Consider an irreversible homodimerization reaction occurring in a small compartment of volume Ω according to the following reaction scheme:

$$\varnothing \xrightarrow{k_1} mX_1,$$

$$X_1 + X_1 \xrightarrow{k_2} X_2,$$

$$X_1 \xrightarrow{k_3} \varnothing,$$

$$X_2 \xrightarrow{k_3} \varnothing.$$

The species X_1 and X_2 represent the monomers and the homodimers, respectively. For simplicity, the decay constants for both species are considered to be equal. Table I shows that only the bimolecular reaction contributes to the vector $\vec{\Delta}$, giving

$$\vec{\Delta} = k_2[\langle \epsilon_1^2 \rangle - \phi_1]\begin{pmatrix} -2 \\ 1 \end{pmatrix}. \tag{27}$$

The deterministic model of the reaction is

$$\frac{\partial \phi_1}{\partial t} = k_1 m - 2k_2\phi_1^2 - k_3\phi_1, \tag{28}$$

$$\frac{\partial \phi_2}{\partial t} = k_2\phi_1^2 - k_3\phi_2, \tag{29}$$

from which it follows that the Jacobian is given by

$$\mathbf{J} = \begin{pmatrix} -4k_2\phi_1 - k_3 & 0 \\ 2k_2\phi_1 & -k_3 \end{pmatrix}. \tag{30}$$

Inserting the matrix $\mathbf{J}$ and the vector $\vec{\Delta}$ in Eq. (26), we obtain

$$\vec{\phi}^R - \vec{\phi} = \frac{k_2\phi_1[1 - \langle \epsilon_1^2 \rangle/\phi_1]}{\Omega(4k_2\phi_1 + k_3)}\begin{pmatrix} 2 \\ -1 \end{pmatrix}. \tag{31}$$

Since the entries of this vector are nonzero, it follows that the true concentrations of both species are generally different than the macroscopic deterministic ones. This is stage 1 of the calculation as outlined in Sec. IV. Note that the deviations are proportional to the Fano factor of species 1 (i.e., $\langle \epsilon_1^2 \rangle / \phi_1$). Since $\langle \epsilon_i^2 \rangle = \phi_i$ for a Poisson distribution, it follows from Eq. (31) that the true concentration of species 1 (2) will be larger (smaller) than the macroscopic concentration if the probability distribution of intrinsic noise of species 1 is sub-Poissonian, i.e., if the width of the probability distribution is smaller than a Poissonian with the same mean. Super-Poissonian behavior would imply the opposite. To find out which of these two possibilities is the case, we need to explicitly compute $\langle \epsilon_1^2 \rangle$. This is stage 2 of the calculation procedure summarized in Sec. IV.

By inspection of the deterministic equations [Eqs. (28) and (29)], it is easily found that the stoichiometric and macroscopic rate function matrices are

$$\mathbf{S} = \begin{pmatrix} m & -2 & -1 & 0 \\ 0 & 1 & 0 & -1 \end{pmatrix}, \quad \mathbf{F} = \begin{pmatrix} k_1 & 0 & 0 & 0 \\ 0 & k_2\phi_1^2 & 0 & 0 \\ 0 & 0 & k_3\phi_1 & 0 \\ 0 & 0 & 0 & k_3\phi_2 \end{pmatrix}. \tag{32}$$

By using the deterministic equations to write ϕ_2 in the above matrices in terms of ϕ_1 and substituting the resultant matrices into the equation $\mathbf{D} = \mathbf{S}\cdot\mathbf{F}\cdot\mathbf{S}^T$ [see point (2) of the stage 2 procedure in Sec. IV], we find the diffusion matrix

$$\mathbf{D} = \begin{pmatrix} k_1 m^2 + k_3\phi_1 + 4k_2\phi_1^2 & -2k_2\phi_1^2 \\ -2k_2\phi_1^2 & 2k_2\phi_1^2 \end{pmatrix}. \tag{33}$$

Substituting the diffusion and Jacobian matrices into Eq. (23) with the left hand side set equal to zero (since we are in steady-state) after some algebraic simplification, we get

$$\langle \epsilon_1^2 \rangle = \phi_1\left(1 - \frac{2k_2\phi_1(2-m) + k_3(1-m)}{2(4k_2\phi_1 + k_3)}\right). \tag{34}$$

Hence, the final explicit equations for the steady-state true concentrations are

$$\vec{\phi}^R = \vec{\phi} + \frac{k_2\phi_1[2k_2\phi_1(2-m)+k_3(1-m)]}{2\Omega(4k_2\phi_1+k_3)^2}\begin{pmatrix}2\\-1\end{pmatrix}. \quad (35)$$

From Eq. (34), we deduce that the probability distribution is sub-Poissonian for $m=1$ and super-Poissonian for $m\geq 2$. As shown in Eq. (35), the consequence of this interesting result is that for $m=1$ the true concentration of species 1 (2) will be larger (smaller) than the macroscopic concentration given by the deterministic equations, whereas the opposite is true for $m\geq 2$. This prediction using the EMRE approach is confirmed (Fig. 1) using Gillespie's SSA (Ref. 4) as implemented in the standard software platform, DIZZY.[12] The steady-state true concentration is obtained from these simulations by averaging over long periods of time and over a large number of independent realizations (for more details, see the caption of Fig. 1). A quantitative test of the numerical accuracy of Eq. (35) is shown in Fig. 2 in which we explore the dependence of the deviations from the predictions of the REs with burst input size m and decay rate k_3. In both cases it can be seen that the EMRE prediction of the true concentration is in good agreement with the results obtained from the SSA; since the latter exactly simulates the stochastic processes described by the master equation, it also follows that the EMRE prediction is in good agreement with the actual solution of the master equation. One of the most useful benefits of the EMRE approach is its ability to predict the region(s) of parameter space in which the solutions of the REs and of master equations differ the most; this is illustrated in Fig. 2(b) where the EMRE correctly predicts that maximum error in the prediction of the RE occurs for decay constants in the range of $k_3=1000-2000$.

We finish this subsection by emphasizing that all expressions that one derives using the EMRE approach will necessarily become quantitatively less accurate as one approaches the limit of small mean numbers of molecules or, equivalently, of very small volumes. A general rule of thumb would be to trust the results only if the average particle numbers are significantly greater than 1; in practice, we have found, to our surprise, that the approximation typically gives good results even when the mean particle numbers are just a little larger than 1 (as, for example, in Fig. 1).

B. Heterodimerization: Bimolecular reactions between different reacting species

Consider an irreversible bimolecular reaction between two different species occurring in a small compartment according to the following reaction scheme:

$$\varnothing \xrightarrow{k_1} mX_1, \quad \varnothing \xrightarrow{k_1} mX_2,$$

$$X_1 + X_2 \xrightarrow{k_2} X_3,$$

$$X_1 \xrightarrow{k_3} \varnothing, \quad X_2 \xrightarrow{k_3} \varnothing, \quad X_3 \xrightarrow{k_3} \varnothing.$$

The species X_1, X_2, and X_3 represent monomers of one kind, monomers of a different kind, and the heterodimers, respectively. For simplicity, the burst input size, import, and decay constants for both species are considered to be equal. Table I shows that only the bimolecular reaction contributes to the vector $\vec{\Delta}$, giving

$$\vec{\Delta} = k_2\langle \epsilon_1\epsilon_2\rangle\begin{pmatrix}-1\\-1\\1\end{pmatrix}. \quad (36)$$

The deterministic model of the reaction is

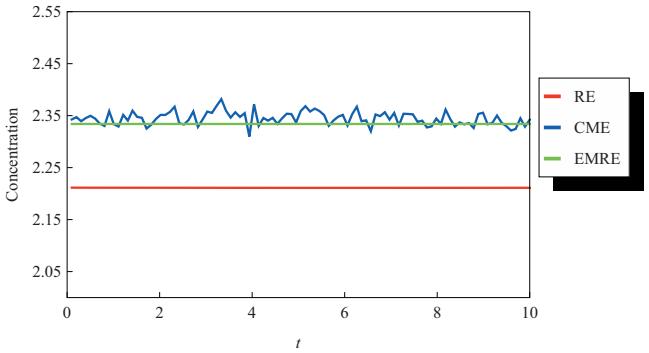

(a) m = 1

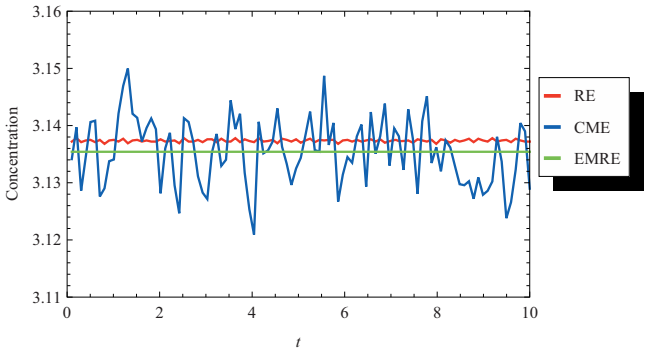

(b) m = 2

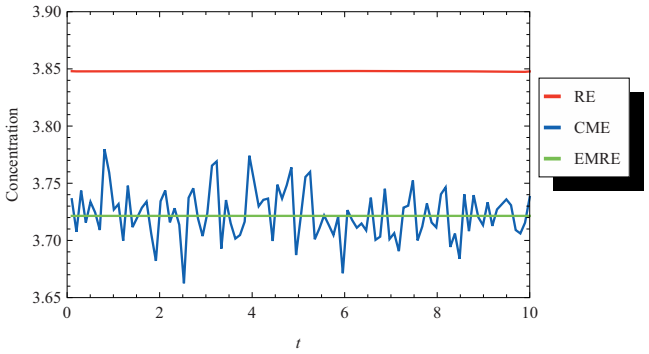

(c) m = 3

FIG. 1. Homodimerization. Plots of the concentration of monomers (particle species 1 in example A) vs time for burst input sizes: (a) $m=1$, (b) $m=2$, and (c) $m=3$. The parameters are $k_1=1000$, $k_2=100$, $k_3=10$, and $\Omega=1$. The graphs compare the concentration of monomers given by the RE, i.e., ϕ_1 (the macroscopic concentration), by the EMRE, i.e., ϕ_1^R (estimate of the true concentration), and by numerically estimating the quantity $\langle n_1\rangle/\Omega$, i.e., the true concentration, from an ensemble average over 10^4 realizations of the stochastic processes described by the CME using Gillespie's SSA. In agreement with predictions based on the theory of EMRE, the true concentration is larger than the macroscopic concentration for $m=1$ and smaller for $m\geq 2$.

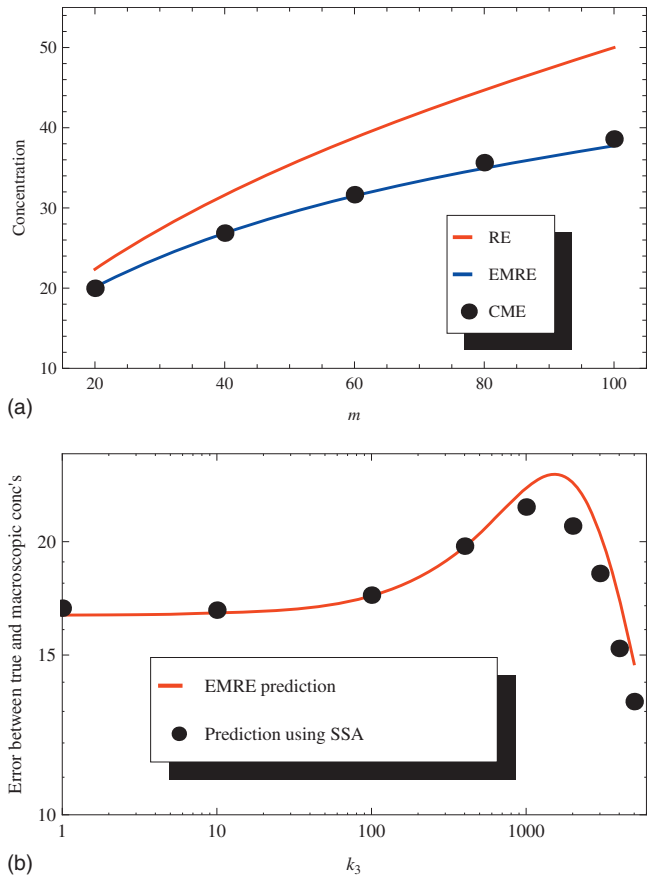

FIG. 2. Homodimerization. (a) Plot of the steady-state concentration of monomers (particle species 1 in example A) vs burst input size m. (b) Plot of the percentage error between the steady-state macroscopic and true concentrations vs the decay constant k_3. (a) shows that as predicted by the EMRE, differences between the true (CME) and macroscopic (RE) concentrations increase with increasing exchange of matter (i.e. with m). As shown in (b), the EMRE also correctly predicts the value of k_3 at which one expects maximum deviation between the true and macroscopic concentrations. Parameter values for (a) are $k_1=2000$, $k_2=40$, $\Omega=1$, and $k_3=1$, while for (b) they are $k_1=1000$, $k_2=40$, $\Omega=1$, and $m=20$. The true concentration is obtained by generating 100 or 1000 SSA realizations of the stochastic processes underlying the CME [for (a) and (b), respectively)], time-averaging the data in each one of these realizations over the time range (0.1,10), and finally ensemble-averaging over all realizations.

$$\frac{\partial \phi_1}{\partial t} = k_1 m - k_2 \phi_1 \phi_2 - k_3 \phi_1, \tag{37}$$

$$\frac{\partial \phi_2}{\partial t} = k_1 m - k_2 \phi_1 \phi_2 - k_3 \phi_2, \tag{38}$$

$$\frac{\partial \phi_3}{\partial t} = k_2 \phi_1 \phi_2 - k_3 \phi_3, \tag{39}$$

from which it follows that the Jacobian is given by

$$\mathbf{J} = \begin{pmatrix} -k_2\phi_2 - k_3 & -k_2\phi_1 & 0 \\ -k_2\phi_2 & -k_2\phi_1 - k_3 & 0 \\ k_2\phi_2 & k_2\phi_1 & -k_3 \end{pmatrix}. \tag{40}$$

Inspection of the steady-state solution of Eqs. (37)–(39) shows that the macroscopic concentrations of species 2 and 3 can be simply written in terms of that of species 1: $\phi_2=\phi_1$ and $\phi_3=k_2\phi_1^2/k_3$. We shall use this substitution in the rest of this example as it simplifies the algebra considerably. Inserting the matrix $\mathbf{J}$ and the vector $\vec{\Delta}$ in Eq. (26) we obtain

$$\vec{\phi}^R - \vec{\phi} = \frac{k_2\langle \epsilon_1 \epsilon_2 \rangle}{\Omega(2k_2\phi_1 + k_3)} \begin{pmatrix} -1 \\ -1 \\ 1 \end{pmatrix}. \tag{41}$$

Once again since all of the entries of this vector are nonzero, it follows that the true concentrations of both species are generally different than the macroscopic concentrations. Next we proceed to stage 2 of the calculation where we explicitly compute $\langle \epsilon_1 \epsilon_2 \rangle$ since this will determine whether the true concentrations are larger or smaller than the macroscopic ones.

The stoichiometric and macroscopic function matrices are found from the deterministic equations to be equal to

$$\mathbf{S} = \begin{pmatrix} m & 0 & -1 & -1 & 0 & 0 \\ 0 & m & -1 & 0 & -1 & 0 \\ 0 & 0 & 1 & 0 & 0 & -1 \end{pmatrix},$$

$$\mathbf{F} = \begin{pmatrix} k_1 & 0 & 0 & 0 & 0 & 0 \\ 0 & k_1 & 0 & 0 & 0 & 0 \\ 0 & 0 & k_2\phi_1^2 & 0 & 0 & 0 \\ 0 & 0 & 0 & k_3\phi_1 & 0 & 0 \\ 0 & 0 & 0 & 0 & k_3\phi_1 & 0 \\ 0 & 0 & 0 & 0 & 0 & k_2\phi_1^2 \end{pmatrix}, \tag{42}$$

from which we obtain the diffusion matrix,

$$\mathbf{D} = \mathbf{S} \cdot \mathbf{F} \cdot \mathbf{S}^T = \begin{pmatrix} k_1 m^2 + k_3\phi_1 + k_2\phi_1^2 & k_2\phi_1^2 & -k_2\phi_1^2 \\ k_2\phi_1^2 & k_1 m^2 + k_3\phi_1 + k_2\phi_1^2 & -k_2\phi_1^2 \\ -k_2\phi_1^2 & -k_2\phi_1^2 & 2k_2\phi_1^2 \end{pmatrix}. \tag{43}$$

Substituting the diffusion and Jacobian matrices into Eq. (23) with the left hand side set equal to zero gives a set of six simultaneous equations in the variables $\langle \epsilon_i \epsilon_j \rangle$ $(i,j=1,\ldots,3)$ but of these only three are needed to get an explicit solution for $\langle \epsilon_1 \epsilon_2 \rangle$,

$$\langle \epsilon_1 \epsilon_2 \rangle = -\frac{k_1 k_2 m^2 \phi_1}{2k_3(2k_2\phi_1 + k_3)}. \tag{44}$$

Since the latter is always negative, it follows from Eq. (41) that the true concentration of species 1 and 2 will be always larger than the macroscopic concentration given by the deterministic equations, while the opposite is true for species 3. We note that to obtain the sign of $\langle \epsilon_1 \epsilon_2 \rangle$ it is in many cases not necessary to fully solve the set of simultaneous equations given by Eq. (23) but rather one tries to express $\langle \epsilon_1 \epsilon_2 \rangle$ in terms of Fano factors. For example, in this particular example, the simultaneous equation corresponding to the {1,2} element of the matrix $\mathbf{J}\cdot\mathbf{C}+\mathbf{C}\cdot\mathbf{J}^T+\mathbf{D}=0$ [i.e., the right hand side of Eq. (23)] gives

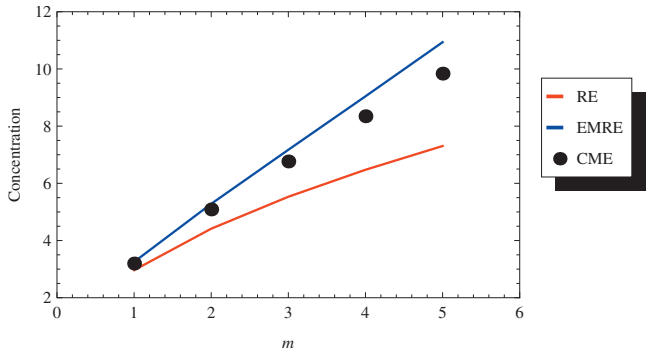

FIG. 3. Heterodimerization. Plot of the steady-state concentration of one of the monomer species (particle species 1 in example B) vs burst input size m. As predicted by EMRE, the true concentration (the first moment of the probability distribution function solution of the CME divided by the volume) is always larger than the macroscopic concentration (solution of the RE) and the difference between the two increases with increasing exchange of matter between the chemical system and its surroundings, i.e., with m. Parameter values are $k_1=500$, $k_2=40$, and $k_3=50$. The true concentration is obtained by generating 1000 SSA realizations of the stochastic processes described by the CME, time-averaging the data in each one of these realizations over the time range (0.1,10), and finally ensemble-averaging over all 1000 realizations.

$$\langle \epsilon_1 \epsilon_2 \rangle = \frac{k_2 \phi_1^2}{2(k_2\phi_1 + k_3)} \left(1 - \frac{\langle \epsilon_1^2 \rangle}{\phi_1} - \frac{\langle \epsilon_2^2 \rangle}{\phi_2} \right). \tag{45}$$

As we showed in the previous example and also in Ref. 6, the burst input process tends to make the Fano factors have values larger than 1. This simply means that the variance of the noise is larger than that expected from a Poisson process, the reason being that in a burst input process one feeds in m molecules at a time, whereas in a Poisson process one feeds into the compartment just one molecule at a time. It follows that $\langle \epsilon_1^2 \rangle / \phi_1$ and $\langle \epsilon_2^2 \rangle / \phi_2$ must have values larger than 1, from which we can deduce that $\langle \epsilon_1 \epsilon_2 \rangle$ is a negative quantity. This procedure may appear superfluous in the context of the present example since in this case we can easily solve for $\langle \epsilon_1 \epsilon_2 \rangle$ [i.e., Eq. (44)] and the expression is simple enough that it can be written compactly and its sign deduced straightforwardly. However, as we shall see in later examples, this particular procedure is very useful when dealing with more complex circuits where the explicit analytical solution of the variables $\langle \epsilon_i \epsilon_j \rangle$ is far too complicated to deduce anything useful from it but in which the present procedure still enables one to obtain the relevant signs.

The final equations for the steady-state true concentrations are

$$\vec{\phi}^R = \vec{\phi} + \frac{k_1 k_2^2 m^2 \phi_1}{2k_3 \Omega (2k_2\phi_1 + k_3)^2} \begin{pmatrix} 1 \\ 1 \\ -1 \end{pmatrix}. \tag{46}$$

The quantitative accuracy of this equation is tested by the SSA using the same methodology as described in the previous example. The results are illustrated in Fig. 3. The true concentration of species 1 is found to be always greater than the macroscopic concentration, exactly as predicted by the EMRE. The deviations become increasingly pronounced with m. The numerical accuracy of the EMRE prediction visibly starts to deteriorate with increasing m as well—this phenomenon is generally true but is particularly obvious in this example compared to the previous one because here we have two input sources rather than the one of the previous example and so the effects of the noise are comparatively much more severe.

C. Enzyme-catalyzed degradation of a cytoplasmic protein

Consider a protein that is constantly being translated from mRNA by ribosomes in the cytoplasm. Experiments have shown that the proteins are generated in bursts where the number of molecules per burst is distributed according to an exponential distribution.[13] In our case, for simplicity, we take the number of molecules per burst to be a constant m. This protein is subsequently degraded through an enzyme-catalyzed reaction operating via the Michaelis–Menten mechanism.[1] These biochemical processes can be modeled by the following set of elementary reactions:

$$\varnothing \xrightarrow{k_1} mP,$$

$$P + E \xrightarrow{k_2} C, \quad C \xrightarrow{k_3} E + P, \quad C \xrightarrow{k_4} E + P_d,$$

$$P_d \xrightarrow{k_5} \varnothing,$$

where P and P_d are the original and degraded forms of the protein respectively, E is the enzyme in its unbound state, and C is the enzyme in its bound state, also called the enzyme-substrate complex. The kinetic description simplifies by noting that we need not describe explicitly the concentrations of complex since the total amount of enzyme is conserved at all times, and hence the concentration of complex is not an independent variable. We denote the original form of the protein as species 1, the free enzyme as species 2, and the degraded form of the protein as species 3. From Table I, we obtain

$$\vec{\Delta} = k_2 \langle \epsilon_1 \epsilon_2 \rangle \begin{pmatrix} -1 \\ -1 \\ 0 \end{pmatrix}. \tag{47}$$

The deterministic model of the reaction is

$$\frac{\partial \phi_1}{\partial t} = k_1 m - k_2 \phi_1 \phi_2 + k_3 (E_T - \phi_2), \tag{48}$$

$$\frac{\partial \phi_2}{\partial t} = -k_2 \phi_1 \phi_2 + (k_3 + k_4)(E_T - \phi_2), \tag{49}$$

$$\frac{\partial \phi_3}{\partial t} = k_4 (E_T - \phi_2) - k_5 \phi_3, \tag{50}$$

where E_T denotes total enzyme concentration which is a constant. It follows that the Jacobian is

$$\mathbf{J} = \begin{pmatrix} -k_2\phi_2 & -k_2\phi_1 - k_3 & 0 \\ -k_2\phi_2 & -(k_2\phi_1 + k_3 + k_4) & 0 \\ 0 & -k_4 & -k_5 \end{pmatrix}. \tag{51}$$

Inserting the matrix $\mathbf{J}$ and the vector $\vec{\Delta}$ in Eq. (26), we obtain

$$\vec{\phi}^R - \vec{\phi} = -\frac{\langle \epsilon_1 \epsilon_2 \rangle}{\Omega \phi_2} \begin{pmatrix} 1 \\ 0 \\ 0 \end{pmatrix}. \tag{52}$$

Note that unlike the previous examples, we now have two entries of this vector being equal to zero, implying that the true free enzyme and degraded protein concentrations will be equal to the corresponding macroscopic concentrations. The fact that this is the case for degraded protein could have been deduced from noting that it is only involved in first-order reactions. However, the result that the true enzyme concentration is unchanged from the macroscopic prediction is quite surprising since the enzyme is involved in a bimolecular reaction. Herein lies the power of stage 1 of the calculation-procedure, i.e., with little effort one can deduce nontrivial results about the true concentrations.

Stage 2 of the calculation gives us expressions for the true concentration of the original protein, which is, in general, different than the macroscopic concentration. The procedure is as in previous examples. From the deterministic equations, we find the stoichiometric and macroscopic rate function matrices,

$$\mathbf{S} = \begin{pmatrix} m & -1 & 1 & 0 & 0 \\ 0 & -1 & 1 & 1 & 0 \\ 0 & 0 & 0 & 1 & -1 \end{pmatrix}, \quad \mathbf{F} = \begin{pmatrix} k_1 & 0 & 0 & 0 & 0 \\ 0 & k_2\phi_1\phi_2 & 0 & 0 & 0 \\ 0 & 0 & k_3(E_T - \phi_2) & 0 & 0 \\ 0 & 0 & 0 & k_4(E_T - \phi_2) & 0 \\ 0 & 0 & 0 & 0 & k_5\phi_3 \end{pmatrix}, \tag{53}$$

which upon substituting into $\mathbf{D} = \mathbf{S} \cdot \mathbf{F} \cdot \mathbf{S}^T$ give us the diffusion matrix,

$$\mathbf{D} = \begin{pmatrix} k_1 m^2 + k_3(E_T - \phi_2) + k_2\phi_1\phi_2 & k_2\phi_1\phi_2 + k_3(E_T - \phi_2) & 0 \\ k_2\phi_1\phi_2 + k_3(E_T - \phi_2) & (k_3 + k_4)(E_T - \phi_2) + k_2\phi_1\phi_2 & k_4(E_T - \phi_2) \\ 0 & k_4(E_T - \phi_2) & k_4(E_T - \phi_2) + k_5\phi_3 \end{pmatrix}. \tag{54}$$

Substituting the diffusion and Jacobian matrices into Eq. (23) with the left hand side set equal to zero and solving three of the six simultaneous equations gives the solution,

$$\langle \epsilon_1 \epsilon_2 \rangle = \frac{2k_4\phi_1\phi_2 - \phi_1(m^2 k_1 + k_4 E_T) - m^2 k_1 K_M}{2k_4(\phi_1 + \phi_2 + K_M)}, \tag{55}$$

where $K_M = (k_3 + k_4)/k_2$ is the Michaelis–Menten constant of the enzyme reaction. By substituting the steady-state solution of the deterministic equations into the above equation, we find that the correlator of the noise of species 1 and 2 is always negative,

$$\langle \epsilon_1 \epsilon_2 \rangle = -\frac{K_M E_T \alpha[\alpha + (1/2)(m-1)]}{K_M + E_T(1-\alpha)^2}, \tag{56}$$

where $\alpha = k_1 m / k_4 E_T$, which is the ratio of the total production rate of original protein and of the maximum rate at which it can be degraded by the enzyme. Hence, it follows that the true steady-state concentration of original protein is always larger than that predicted by the macroscopic equations,

$$\vec{\phi}^R = \vec{\phi} + \frac{\alpha}{\Omega(1-\alpha)} \frac{K_M[\alpha + (1/2)(m-1)]}{K_M + E_T(1-\alpha)^2} \begin{pmatrix} 1 \\ 0 \\ 0 \end{pmatrix}. \tag{57}$$

From the definition of α, it can be deduced that as it approaches the value of 1, the enzyme becomes saturated with substrate; Eq. (57) shows that it is in this saturation limit that the differences between true and macroscopic concentrations become very significant. Simulations (see Fig 4) verify the latter prediction as well as the previous prediction that the steady-state true concentrations of degraded protein and of enzyme are the same as those predicted by the deterministic equations.

D. Catalysis via sequential enzyme reactions

Consider the two-step enzyme catalysis of a substrate S_1 which is input into a compartment. The substrate is converted into an intermediate S_2 via enzyme E_1. The intermediate serves as a substrate for a different enzyme E_2, leading

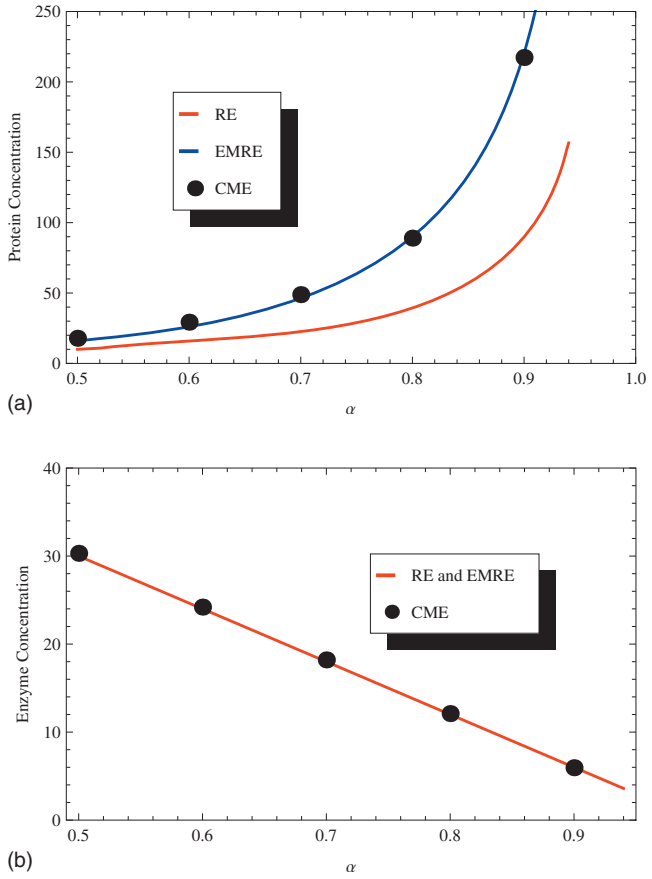

FIG. 4. Enzyme-catalyzed degradation of protein. Plots of the steady-state concentration of the protein species (a) and of the steady-state concentration of enzyme (b) vs the dimensionless parameter α. The latter is a measure of how close is the enzyme to saturation conditions. As predicted by EMRE, (a) the deviations between the true concentration (the first moment of the probability distribution function solution of the CME divided by the volume) and of the macroscopic protein concentration (as predicted by the RE) increases as one approaches saturation; (b) the steady-state true and macroscopic concentrations for enzyme agree exactly. Parameters are $k_2=4$, $k_3=3$, $k_4=37$, $k_5=10$, $\Omega=1$, $m=30$, and $E_T=60$. The parameter α is varied from 0 to 1 by varying the value of k_1. The true concentration is obtained by generating 100 SSA realizations of the stochastic processes underlying the CME, time-averaging the data in each one of these realizations over the time range (10,100), and finally ensemble-averaging over all 100 realizations.

to production of the final product S_3. The latter is then transported out of the compartment. The set of elementary reactions describing this overall process are

$$\emptyset \xrightarrow{k_1} mS_1,$$

$$S_1 + E_1 \xrightarrow{k_2} C_1, \quad C_1 \xrightarrow{k_3} E_1 + S_1, \quad C_1 \xrightarrow{k_4} E_1 + S_2,$$

$$S_2 + E_2 \xrightarrow{k_5} C_2, \quad C_2 \xrightarrow{k_6} E_2 + S_2, \quad C_2 \xrightarrow{k_7} E_2 + S_3,$$

$$S_3 \xrightarrow{k_8} \emptyset .$$

As in the previous example, the complex concentrations are not independent variables and hence need not be explicitly included in our description. Labeling S_1, E_1, S_2, E_2, and S_3 as species 1, 2, 3, 4, and 5, respectively, we can write the following deterministic equations:

$$\frac{\partial \phi_1}{\partial t} = k_1 m - k_2 \phi_1 \phi_2 + k_3 (E_{T1} - \phi_2), \tag{58}$$

$$\frac{\partial \phi_2}{\partial t} = -k_2 \phi_1 \phi_2 + (k_3 + k_4)(E_{T1} - \phi_2), \tag{59}$$

$$\frac{\partial \phi_3}{\partial t} = k_4 (E_{T1} - \phi_2) - k_5 \phi_3 \phi_4 + k_6 (E_{T2} - \phi_4), \tag{60}$$

$$\frac{\partial \phi_4}{\partial t} = -k_5 \phi_3 \phi_4 + (k_6 + k_7)(E_{T2} - \phi_4), \tag{61}$$

$$\frac{\partial \phi_5}{\partial t} = k_7 (E_{T2} - \phi_4) - k_8 \phi_5, \tag{62}$$

where E_{T1} and E_{T2} denote total enzyme concentration of enzymes E_1 and E_2, respectively. The Jacobian can be computed from the deterministic equations and the vector $\vec{\Delta}$ using Table I, as in previous examples. Substituting these two into Eq. (26), we obtain

$$\vec{\phi}^R - \vec{\phi} = -\frac{1}{\Omega} \begin{pmatrix} \langle \epsilon_1 \epsilon_2 \rangle \phi_2^{-1} \\ 0 \\ \langle \epsilon_3 \epsilon_4 \rangle \phi_4^{-1} \\ 0 \\ 0 \end{pmatrix}. \tag{63}$$

Hence, we deduce that the true concentrations of both enzymes (species 2 and 4) and of the final product (species 5) are equal to the macroscopic concentrations. These results are essentially generalizations of the previous example and can be extended straightforwardly to a sequential chain of any number of enzyme-catalyzed reactions.

As in previous examples, one proceeds by computing the stoichiometric and macroscopic rate functions from which one obtains the diffusion matrix $\mathbf{D}$. Substituting the latter and the Jacobian matrix into Eq. (23) with the left hand side equal to zero, one gets a set of 15 simultaneous equations for the variables $\langle \epsilon_i \epsilon_j \rangle$ $(i,j=1,\ldots,5)$. These equations can be easily solved numerically; however, because of their sheer large number, it is to be expected that a compact analytical solution is generally not possible. However, we can, with relative ease, deduce the sign of $\langle \epsilon_1 \epsilon_2 \rangle$ and $\langle \epsilon_3 \epsilon_4 \rangle$ with the method introduced in the example on heterodimerization. The crucial idea is to use the simultaneous equations to express the latter correlators in terms of the relevant Fano factors. Using the two simultaneous equations corresponding to the {2,2} and {4,4} elements of the matrix $\mathbf{J}\cdot\mathbf{C}+\mathbf{C}\cdot\mathbf{J}^T+\mathbf{D}=0$, we, respectively, get

$$\langle \epsilon_1 \epsilon_2 \rangle = K_{M1} \left(\left[1 - \frac{\langle \epsilon_2^2 \rangle}{\phi_2} \right] \left(\frac{E_{T1} - \phi_2}{\phi_2} \right) - \frac{\langle \epsilon_2^2 \rangle}{\phi_2} \right), \tag{64}$$

$$\langle \epsilon_3 \epsilon_4 \rangle = K_{M2} \left(\left[1 - \frac{\langle \epsilon_4^2 \rangle}{\phi_4} \right] \left(\frac{E_{T2} - \phi_4}{\phi_4} \right) - \frac{\langle \epsilon_4^2 \rangle}{\phi_4} \right). \tag{65}$$

Since the burst input mechanism will push the Fano factors to be larger than unity, it follows that the above correlators

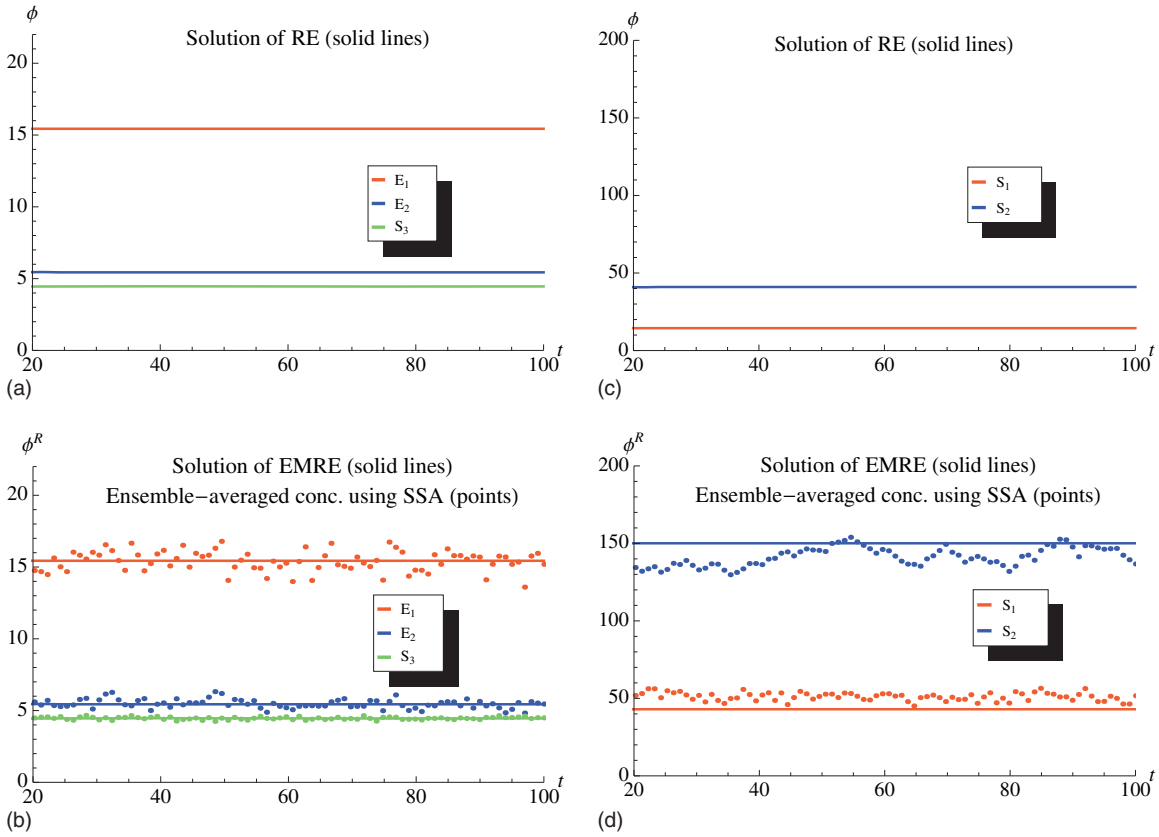

FIG. 5. Sequential enzyme-catalyzed reactions. Plots of the concentration of the enzyme and substrate protein species vs time. A comparison of (a) and (b) shows that the true and macroscopic concentrations (i.e., ensemble-averaged concentration from SSA and RE predictions, respectively) are the same for all enzyme species (E_1, E_2) and for one protein species (S_3). In contrast, a comparison of (c) and (d) shows that the true and macroscopic concentrations are very different for two protein species (S_1 and S_2). Note how the differences between the two concentrations are very well predicted by the EMRE. Parameters are $k_1=12.7$, $k_2=2$, $k_3=0$, $k_4=10$, $k_5=2$, $k_6=0$, $k_7=10$, $k_8=100$, $\Omega=1$, $m=35$, $E_{T1}=60$, and $E_{T2}=50$. The true concentration is obtained by ensemble-averaging over 500 SSA realizations of the stochastic processes described by the CME.

are generally negative; consequently, by Eq. (63) the true concentrations of species 1 and 3 have to be larger than the macroscopic concentrations.

Stochastic simulation confirms that as predicted by Eq. (63), the true enzyme and product concentrations are equal to the macroscopic concentrations [compare Figs. 5(a) and 5(b)], while the true substrate concentrations are significantly larger than the macroscopic ones [compare Figs. 5(c) and 5(d)]. In Fig. 5(d) we also show that the numerical solution of the EMRE (solid lines) agrees very well with the ensemble-averaged number density obtained from the SSA using DIZZY. It is interesting to note that using a single machine with a 3.0 GHz processor, the numerical solution of the EMRE (using MAPLE 9.5) takes just few seconds compared to about 1.5 min using DIZZY's implementation of the SSA. Hence, the EMRE approach is also promising as an efficient numerical means of estimating the first moments of the probability distribution function solution of the CME—this is discussed more fully in a separate forthcoming publication.

E. Positive feedback loops

In this last example we treat the case where there exists a feedback loop in our biochemical circuit and use the EMRE method to infer how such loops influence the differences between the predictions of REs and CMEs. Consider a chemical circuit in which a substrate protein fed into a compartment is converted into some other protein via three intermediate stages and in which there is a positive feedback loop. The conversion of one substrate to another occurs through enzyme catalysis. The loop is between the protein initially fed into the compartment and one of the other proteins. Thus, for a circuit composed of four distinct interchanging substrate proteins there are three distinct configurations (Fig. 6).

The superscript over the arrows in the above reactions denote the enzyme which catalyzes the process: the conversion of species S_i to S_{i+1} is effected through an enzyme E_i where i is an index taking values between 1 and 3, while the conversion associated with the positive feedback loop is via enzyme E_4. The detailed reaction scheme showing all elementary chemical reactions is needed for our analysis,

$$\varnothing \xrightarrow{k_{\text{in}}} mS_1,$$

$$S_1 + E_1 \underset{k_1}{\overset{k_0}{\rightleftharpoons}} C_1 \xrightarrow{k_2} S_2 + E_1,$$

$$S_2 + E_2 \underset{k_1}{\overset{k_0}{\rightleftharpoons}} C_2 \xrightarrow{k_2} S_3 + E_2,$$

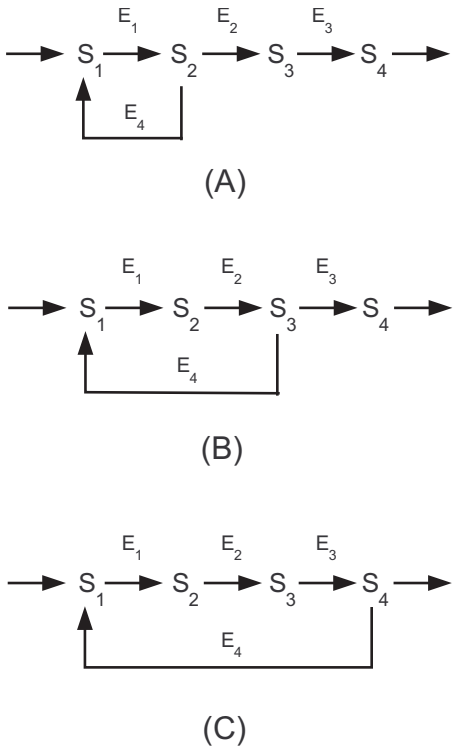

FIG. 6. Positive feedback loop Schematic illustrating the three possible configurations of a chemical circuit composed of 4 distinct interchanging substrate proteins with one positive feedback loop. Protein fed into a compartment is converted into some other protein via three intermediate stages; the conversion of one protein to another occurs through enzyme catalysis. The loop is between the protein initially fed into the compartment and one of the other proteins. The substrate proteins and enzymes are labeled S_i and E_i, respectively.

$$S_3 + E_3 \underset{k_1}{\overset{k_0}{\rightleftharpoons}} C_3 \overset{k_2}{\rightarrow} S_4 + E_3,$$

$$X + E_4 \underset{k_1}{\overset{k_0}{\rightleftharpoons}} C_4 \overset{k_2}{\rightarrow} S_1 + E_4,$$

$$S_4 \overset{k_{\text{out}}}{\rightarrow} \varnothing .$$

where X denotes S_2 for circuit A, S_3 for circuit B, and S_4 for circuit C. Note that the total amount of enzyme for each of the four species is not assumed to be the same. The kinetics of each one of these circuits can be described in terms of eight distinct chemical species, i.e., E_1, E_2, E_3, E_4, S_1, S_2, S_3, and S_4 which we relabeled as $\phi_1, \phi_2, \ldots, \phi_8$, respectively. A "stage 1" analysis of the circuits gives the following results:

$$\text{Circuit A: } \vec{\phi}^R - \vec{\phi} = \frac{1}{\Omega}\left(\frac{\phi_4}{\phi_2}\langle \epsilon_2 \epsilon_6 \rangle - \langle \epsilon_4 \epsilon_6 \rangle\right)(\phi_6 + K_M)^{-1} \times \begin{pmatrix} 1 \\ 0 \\ 0 \\ 1 \end{pmatrix}, \quad (66)$$

$$\text{Circuit B: } \vec{\phi}^R - \vec{\phi} = \frac{1}{\Omega}\left(\frac{\phi_4}{\phi_3}\langle \epsilon_3 \epsilon_7 \rangle - \langle \epsilon_4 \epsilon_7 \rangle\right)(\phi_7 + K_M)^{-1} \times \begin{pmatrix} 1 \\ 1 \\ 0 \\ 1 \end{pmatrix}, \quad (67)$$

$$\text{Circuit C: } \vec{\phi}^R - \vec{\phi} = -\frac{1}{\Omega}\langle \epsilon_4 \epsilon_8 \rangle (\phi_8 + K_M)^{-1} \begin{pmatrix} 1 \\ 1 \\ 1 \\ 1 \end{pmatrix}, \quad (68)$$

where $K_M = (k_1 + k_2)/k_0$ is the Michaelis–Menten constant of the enzyme reactions. Note that we are focusing on the enzyme species, and hence in the above equations, we do not show the vector entries for the substrate protein components. The most notable feature of this analysis is that only those enzymes inside the overall feedback loop have true concentrations different than macroscopic predictions. For example, for circuit A, only enzymes E_2 and E_3 are outside the closed feedback loop (Fig. 6), and hence it is only for these that the true and macroscopic concentrations agree. It is also interesting to note that even though we have different amounts of total enzyme of each species, the difference between true and macroscopic concentrations is the same for all enzymes in a circuit. A similar analysis for the substrate protein components shows that for all circuits, the true concentrations of S_1, S_2, and S_3 are different than the macroscopic concentrations, while that of S_4 is the same. Simulation results (data not shown) confirm that all species which were identified by stage 1 of the EMRE analysis as having equal true and macroscopic concentrations do actually possess this property.

We finish this section by emphasizing that a stage 1 analysis can only identify the minimum number of species whose true concentration matches the macroscopic one; some species which at this stage of the calculation are associated with a nonzero element in the vector $\vec{\phi}^R - \vec{\phi}$ could still evaluate to zero (or to a negligibly small value) in stage 2 of the calculation.

VI. CONCLUSION

In this article, we have presented a new formalism, EMREs, which can be seen as extensions of the conventional REs to describing chemical kinetics at mesoscopic spatial scales. The EMREs were formally derived from the CME using the system-size expansion including terms of the order of $\Omega^{-1/2}$. The fact that the true concentrations obey a different RE than the macroscopic equations implies that intrinsic noise induces a renormalization of the concentrations; this phenomenon is due to terms in the system-size expansion which are beyond the conventional linear-noise approximation of CMEs, i.e., the system-size expansion including terms of the order of Ω^0 and, consequently, also beyond the Fokker–Planck equation. Indeed, we have shown that the time evolution of the joint probability distribution function of the mesoscopic system obeys a more general equation than the Fokker–Planck equation.

We note that while the EMRE is not the only effective RE whose solution approximates the true concentrations (see, for example, Refs. 14 and 15), it is the only one, to our knowledge, which is derived from a systematic expansion method. Other types of effective REs in the literature are based on moment-closure methods, i.e., one writes down an infinite system of equations for the moments (directly from the master equations) and then one truncates by some closure rule. The choice of such rules is arbitrary and the accuracy of the approximation is expected to depend strongly on the dynamics of the system.[5,16] The formulation of the system-size expansion by Van Kampen was indeed spurred by the need to have a systematic method of approximating master equations rather than an ad hoc prescription for cutting off the higher moments of fluctuations. The EMRE formalism being derived from the same system-size expansion enjoys the same advantage. In particular, from Eq. (26) it follows that our estimates of the true concentrations are accurate to order Ω^{-1}.

Interestingly, we have found that the differences between the true concentrations (the first moments of the probability distribution function solution of the CME divided by the compartment volume) and the macroscopic concentrations (the solutions of the REs) grows with the Fano factors of the system, a common measure of the non-Poissonian nature of fluctuations. We have also shown through a series of biochemical examples that the true concentrations can have smaller (e.g., a homodimerization reaction), larger (e.g., a heterodimerization reaction), or the same (e.g., a simple-enzyme reaction) values as the macroscopic concentrations. It is common, if not the norm, that the true concentration of one species in a system will be larger than the corresponding macroscopic concentration while that of another species in the same system will be the same or less than the macroscopic: the sign and magnitude of the deviations from macroscopic prediction are a sensitive function of the precise topology of the chemical network. Even for large systems, stage 1 of the EMRE calculation enables one to deduce, with little effort, all species whose true and macroscopic concentrations are equal. For small systems, stage 2 enables one to deduce explicit expressions for the steady-state true concentrations. For large systems, this is not feasible and numerical solution of EMREs becomes indispensable; this is not surprising since for such systems one cannot even find analytical solutions of the REs. Preliminary tests show that even for relatively large systems, EMREs may provide a quick and efficient numerical means to map out the regions of parameter space characterized by maximum differences between the predictions of the stochastic and deterministic models of biochemical kinetics. The EMRE formalism was specifically derived for the case of reactions occurring in a well-mixed compartment—an extension of the formalism to the case of mesoscopic, spatially inhomogeneous systems maybe possible by constructing a set of differential equations whose solution approximates the true concentrations as given by the reaction-diffusion master equation.[17,18]

ACKNOWLEDGMENTS

It is a pleasure to thank Christian Fleck for stimulating discussions. Support from SULSA (Scottish Universities Life Sciences Alliance) is gratefully acknowledged.

[1] A. Cornish-Bowden, *Fundamentals of Enzyme Kinetics* (Portland, London, 1995).
[2] R. Grima and S. Schnell, Essays Biochem. **45**, 41 (2008).
[3] D. T. Gillespie, Annu. Rev. Phys. Chem. **58**, 35 (2007).
[4] D. T. Gillespie, J. Phys. Chem. **81**, 2340 (1977).
[5] N. G. Van Kampen, *Stochastic Processes in Physics and Chemistry* (Elsevier, Amsterdam, 2007).
[6] J. Elf and M. Ehrenberg, Genome Res. **13**, 2475 (2003).
[7] R. Grima, Phys. Rev. Lett. **102**, 218103 (2009).
[8] R. Grima, BMC Syst. Biol. **3**, 101 (2009).
[9] I. M. Jaimoukha and E. M. Kasenally, SIAM (Soc. Ind. Appl. Math.) J. Numer. Anal. **31**, 227 (1994).
[10] P. Benner, V. Sima, and M. Slowik, J. Numer. Anal. Indust. Appl. Math **2**, 11 (2007).
[11] B. Alberts, D. Bray, J. Lewis, M. Raff, K. Roberts, and J. D. Watson, *Molecular Biology of the Cell* (Garland, New York, 1994).
[12] S. Ramsey, D. Orrell, and H. Bolouri, J. Bioinf. Comput. Biol. **3**, 415 (2005).
[13] L. Cai, N. Friedman, and X. S. Xie, Nature (London) **440**, 358 (2006).
[14] A. Singh and J. P. Hespanha, Proceedings of the 45th Conference on Decision and Control, 2006.
[15] C. A. Gómez-Uribe and G. C. Verghese, J. Chem. Phys. **126**, 024109 (2007).
[16] S. A. Levin and S. W. Pacala, in *Spatial Ecology: The Role of Space in Population Dynamics and Interspecific Interactions*, edited by D. Tilman and P. Kareiva (Princeton University Press, Princeton, NJ, 1997), pp. 271–296.
[17] F. Baras and M. Malek Mansour, Phys. Rev. E **54**, 6139 (1996).
[18] D. Bernstein, Phys. Rev. E **71**, 041103 (2005).